



DogFit: Domain-guided Fine-tuning for Efficient Transfer Learning of Diffusion Models*

Yara Bahram¹, Mohammadhadi Shateri¹, Eric Granger¹

¹LIVIA, Dept. of Systems Engineering, ÉTS Montreal, Canada
yara.mohammadi-bahram@livia.etsmtl.ca, {mohammadhadi.shateri, eric.granger}@etsmtl.ca

Abstract

Transfer learning of diffusion models to smaller target domains is challenging, as naively fine-tuning the model often results in poor generalization. Test-time guidance methods help mitigate this by offering controllable improvements in image fidelity through a trade-off with sample diversity. However, this benefit comes at a high computational cost, typically requiring dual forward passes during sampling. We propose the Domain-guided Fine-tuning (DogFit) method, an effective guidance mechanism for diffusion transfer learning that maintains controllability without incurring additional computational overhead. DogFit injects a domain-aware guidance offset into the training loss, effectively internalizing the guided behavior during the fine-tuning process. The domain-aware design is motivated by our observation that during fine-tuning, the unconditional source model offers a stronger marginal estimate than the target model. To support efficient controllable fidelity–diversity trade-offs at inference, we encode the guidance strength value as an additional model input through a lightweight conditioning mechanism. We further investigate the optimal placement and timing of the guidance offset during training and propose two simple scheduling strategies, i.e., *late-start* and *cut-off*, which improve generation quality and training stability. Experiments¹ on DiT and SiT backbones across six diverse target domains show that DogFit can outperform prior guidance methods in transfer learning in terms of FID and FD_{DINOv2} while requiring up to 2x fewer sampling TFLOPS.

Introduction

Denosing diffusion probabilistic models (DDPMs) (Sohl-Dickstein et al. 2015; Ho, Jain, and Abbeel 2020) have emerged as powerful generative models, achieving state-of-the-art (SOTA) results in image synthesis (Dhariwal and Nichol 2021; Rombach et al. 2022), video generation (Gupta et al. 2024; Ho et al. 2022), and image editing (Kawar et al. 2023). However, producing high-quality and diverse outputs still requires substantial computational and data resources, particularly with large diffusion backbones and image sizes. In practical applications such as personalized generation with limited data, full model training from scratch is

*This paper is currently under review.

Copyright © 2026, Association for the Advancement of Artificial Intelligence (www.aaai.org). All rights reserved.

¹Code will be made public upon acceptance.

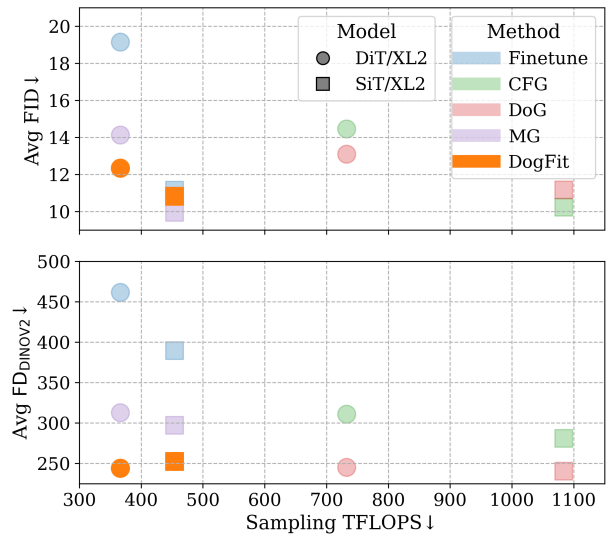


Figure 1: DogFit achieves competitive average FID and FD_{DINOv2} when compared to SOTA guidance mechanisms for diffusion transfer learning, all without increasing the computational complexity (sampling TFLOPS).

infeasible, making transfer learning a critical tool for target adaptation. A common approach in this setting is to fine-tune a pre-trained diffusion model on the target data. While straightforward, this strategy frequently suffers from overfitting and poor generalization due to the limited size and diversity of the target domain.

Classifier-free guidance (CFG) is a standard technique for improving generation quality at inference time by modulating the conditional signal (Ho and Salimans 2022; Karras et al. 2024). This technique is often used in its original form even after target adaptation to steer the model towards better generalization. However, CFG assumes access to well-trained conditional and unconditional models, which is difficult to ensure in transfer scenarios where the target domain is small or lacks labels (Ho and Salimans 2022; Zhong et al. 2025). Recent methods like domain guidance (DoG) address these issues by utilizing the unconditional source model as a

stronger marginal noise estimator, offering improved target domain alignment and generalization (Zhong et al. 2025; Phunyaphibarn et al. 2025). Nevertheless, both CFG and DoG introduce significant computational overhead at sampling time due to their reliance on dual forward passes (Ho and Salimans 2022; Zhong et al. 2025). On the other hand, model guidance (MG) mitigates CFG’s runtime cost in in-domain settings by injecting the guidance signal directly into the diffusion training objective (Chen et al. 2025; Tang et al. 2025). However, MG inherits the limitations of CFG in transfer learning and hard-codes the guidance strength value during training, restricting control at inference. These limitations raise a key question: *can we design effective guidance mechanisms for diffusion transfer learning without incurring computational overhead and still maintaining controllability over the guidance strength?*

This paper proposes domain-guided fine-tuning (DogFit), a method that injects a domain-aware guidance offset into the training loss during the fine-tuning process. This allows the diffusion model to directly learn the guided direction, removing the need for additional test-time processes. The domain-aware design is motivated by our observation that during fine-tuning, the source model offers stronger marginal noise estimates than the evolving target model. This design encourages the model to step toward the target domain manifold and avoid out-of-distribution generation. To support efficient control over the guidance strength at inference, DogFit conditions the model on the guidance value and exposes it to a range of such values during training. This allows the model to modulate its generation behavior accordingly, enabling fidelity–diversity trade-offs at inference with negligible sampling overhead. We further investigate the optimal placement and timing of the guidance offset during training. Two cost-effective guidance scheduling mechanisms are proposed for DogFit: (1) a *late-start* strategy that delays guidance until the model has learned sufficiently stable target representations; and (2) a *cut-off* scheme that restricts guidance to the later denoising steps, where fine-grained domain-specific details are more prevalent. Results over six datasets with different distribution shifts and supervision levels, using two SOTA diffusion backbones, DiT (Peebles and Xie 2023) and SiT (Ma et al. 2024), show that DogFit can outperform SOTA guidance methods in terms of FID and FD_{DINOv2} while reducing their sampling TFLOPS by up to 2× (see Figure 1). Results establish DogFit as a practical and efficient guidance method for diffusion transfer learning.

Our contributions are as follows:

- We propose DogFit, a training-time guidance mechanism for diffusion transfer learning that enables controllable improvement over target domain generation fidelity without requiring additional processes or double forward passes at test-time.
- We show that, during fine-tuning, the source domain model offers stronger marginal estimates than the target model, making it better suited for generating guidance signals. We empirically analyze how the timing and placement of this guidance impact training and propose

two scheduling strategies that enhance training stability and generation quality.

- Extensive experiments are conducted across diverse target datasets on DiT and SiT diffusion backbones, showing that DogFit can outperform SOTA guidance methods in transfer learning.

Related Work

Efficient Diffusion Models. The iterative denoising process in diffusion models imposes high sampling-time costs (Shen et al. 2025). To accelerate generation, prior work reduces the number of sampling steps via improved solvers (Song, Meng, and Ermon 2020; Lu et al. 2022), optimized noise schedules (Zheng et al. 2023), or distillation-based methods that train few(one)-step student models to mimic large multi-step teachers (Salimans and Ho 2022; Yin et al. 2024). Recent efforts (Jensen and Sadat 2025; Hsiao et al. 2024; Zhou et al. 2025) distill CFG to eliminate test-time dual passes. Our method, similar to CFG distillation, aims to internalize guidance, but does so without the architectural modifications or post-hoc training stages required by distillation methods. Instead, DogFit simply integrates guidance directly into the fine-tuning objective.

Diffusion Transfer Learning. Transfer learning adapts a model pre-trained on a large-scale source domain to a target domain with smaller size and diversity, leveraging learned representations for better generalization (Weiss, Khoshgof-taar, and Wang 2016). In the context of diffusion models, strategies broadly fall into three categories: Parameter-efficient fine-tuning (PEFT) methods reduce training cost by limiting the number of trainable parameters, often via adapters or LoRA (Guo, Rush, and Kim 2020; Xie et al. 2023; Moon et al. 2022). Distillation-based methods preserve pre-trained source priors during adaptation, particularly during early denoising steps (Zhong et al. 2024; Hur et al. 2024). Few-shot image generation methods enable unconditional diffusion models to generalize to unseen domains using as few as 10 target images (Zhu et al. 2022; Wang et al. 2024; Cao and Gong 2024; Ouyang et al. 2024). Despite this progress, current methods overlook the role of guidance in shaping the generation trajectory, implicitly assuming that its original form remains optimal after adaptation, a limiting assumption in small, low-diversity target domains. We propose a new guidance method tailored for diffusion transfer that can be layered on top of existing fine-tuning methods for improving generalization without incurring additional sampling cost.

Proposed Method

Let ϵ_{θ_0} denote a diffusion model pre-trained on a large-scale source domain \mathcal{D}^S , and let \mathcal{D}^T be a smaller target domain such that $|\mathcal{D}^T| \ll |\mathcal{D}^S|$ (typically, $1000 < |\mathcal{D}^T|$). The goal of transfer learning is to fine-tune a model ϵ_{θ} (initialized with the weights θ_0 of the pre-trained model) on \mathcal{D}^T such that it generates high-quality, diverse samples aligned with the target distribution $p(x|\mathcal{D}^T)$. In this work, we aim to develop a strong guidance mechanism for diffusion transfer

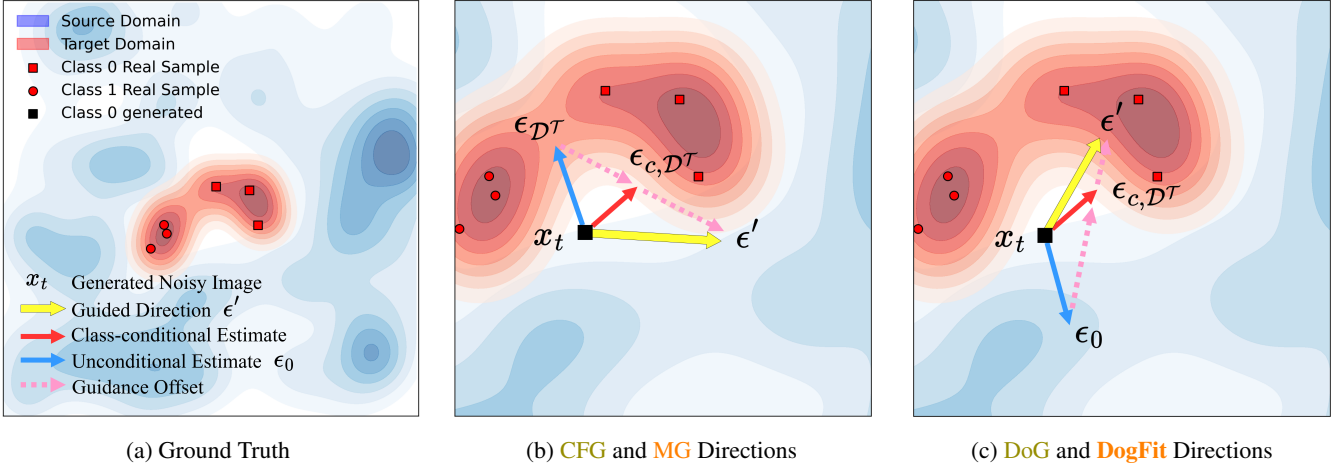


Figure 2: Illustration of transfer learning via guidance mechanisms for synthetic data created using a mixture of Gaussian distributions. (a) The red region defines the target domain, while the blue background represents the source distribution. (b) CFG and MG prioritize class separability without considering the source distribution, often pushing samples toward out-of-distribution areas in the target domain. (c) **DoG** and **DogFit** utilize source information to emphasize movement towards the core of the target manifold, improving domain alignment. (*) **Sampling-time** guidance methods (DoG and CFG) operate by computing the **guidance offset**, whereas **training-time** guidance methods (**DogFit** and MG) learn the **guided direction** directly.

learning that is computationally efficient and supports controllable guidance strength.

Preliminaries

Diffusion Models. Denoising Diffusion Probabilistic Models (DDPMs) (Ho, Jain, and Abbeel 2020) are generative models that learn to reverse a fixed noising process applied over T time-steps. Starting from a clean image x_0 , noise is gradually added to produce a sequence of noisy images $\{x_t\}_{t=1}^T$. A neural network $\epsilon_\theta(x_t, t)$ is trained to predict the noise ϵ at each time-step t , using this denoising objective:

$$\mathcal{L}_{\text{simple}} = \mathbb{E}_{t, x_0, \epsilon} [\|\epsilon_\theta(x_t, t) - \epsilon\|^2]. \quad (1)$$

Time step t is omitted in subsequent equations when it is clear from context. In conditional generation, the model receives an auxiliary input c (e.g., class labels or text), producing $\epsilon_\theta(x_t | c)$. SOTA transformer-based diffusion architectures such as DiT (Peebles and Xie 2023) and SiT (Ma et al. 2024) operate in latent space rather than directly on pixel space. For notational simplicity, however, we keep using x to denote the model input.

Guidance in Transfer Learning. While diffusion models can functionally incorporate conditional inputs during training, their outputs often drift under weak conditioning, motivating the use of guidance signals during the reverse process (Dhariwal and Nichol 2021; Ho and Salimans 2022). We present three representative guidance strategies in transfer learning (i.e., CFG, MG, and DoG) covering the main design axes: *where* the guidance signal originates (unconditional branch, or external source model) and *when* it is injected (sampling-time vs. training-time) (See Figure 2 for a visual comparison).

- *Classifier-Free Guidance (CFG)* (Ho and Salimans 2022; Nichol et al. 2021) improves conditional generation by extrapolating the model’s class-conditional prediction further away from its unconditional counterpart—typically using the same model. The reverse process is modified as:

$$\epsilon'_\theta(x_t | c) = \epsilon_\theta(x_t | c) + (w - 1) \cdot (\epsilon_\theta(x_t | c) - \epsilon_\theta(x_t)), \quad (2)$$

where increasing the guidance scale $w > 1$ amplifies the effect of the condition during sampling. CFG poses limitations in transfer settings: The unconditional noise estimator is prone to underfitting due to joint training under limited target training data (Chen et al. 2023). Further, CFG often steers generations toward out-of-distribution regions in the target domain (see Figure 2 (b)), and it relies on conditionally labeled data, which may be unavailable in some domains (Zhong et al. 2025).

- *Domain Guidance (DoG)* (Zhong et al. 2025) offers a stronger alternative in transfer learning by using the unconditional source model as the marginal noise estimator:

$$\epsilon'_\theta(x_t | c, \mathcal{D}^T) = \epsilon_\theta(x_t | c, \mathcal{D}^T) + (w - 1) \cdot (\epsilon_\theta(x_t | c, \mathcal{D}^T) - \epsilon_{\theta_0}(x_t)), \quad (3)$$

where $\epsilon^{\text{DoG}}(x_t | c, \mathcal{D}^T)$ is the fine-tuned target model’s class-conditional prediction and $\epsilon_{\theta_0}(x_t)$ is the unconditional one of the source model. The source model, having been trained on rich data, provides a stronger reference point than CFG and further improves target domain alignment (Zhong et al. 2025) (see Figure 2 (c)). Like CFG, however, DoG requires two forward passes during sampling.

- *Model Guidance (MG)* (Tang et al. 2025) removes the need for CFG-style computation during sampling by incorporating its effect directly into the training objective. The model

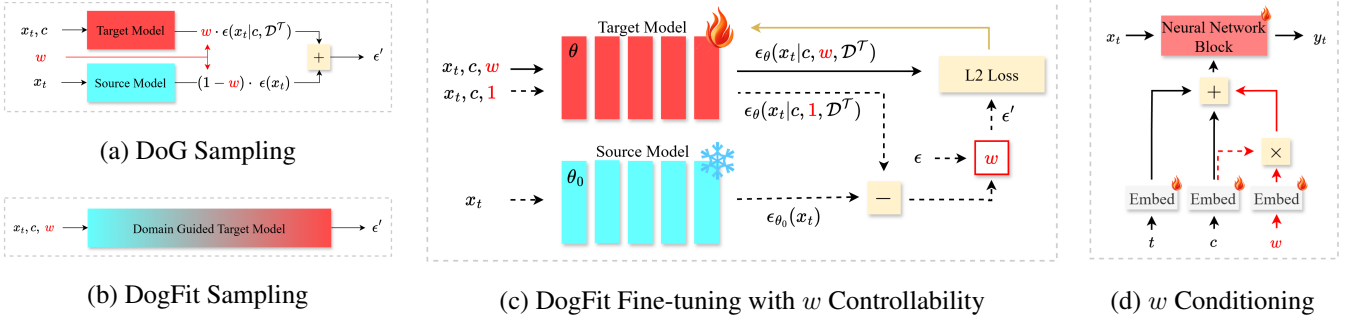


Figure 3: Visual illustration of DogFit during training and sampling : (a–b) DogFit internalizes guidance behavior, removing the need for inference-time double forward passes. (c) During training, the guidance value is treated as an input, allowing inference-time control. The simple case of our method, with fixed guidance, simply requires removing the w and 1 from the target model conditions. (d) w is embedded it as an extra input during fine-tuning, allowing inference-time control. (*) Dashed lines denote paths that do not propagate gradients.

is trained to match a guidance-enhanced noise target:

$$\begin{aligned} \mathcal{L}_{\text{MG}} &= \mathbb{E}_{t, (x_0, c), \epsilon} \|\epsilon_{\theta}(x_t | c) - \epsilon'\|^2, \\ \epsilon' &= \epsilon + (w - 1) \cdot \text{sg}(\epsilon_{\theta}(x_t | c) - \epsilon_{\theta}(x_t)), \end{aligned} \quad (4)$$

where $\text{sg}(\cdot)$ denotes the stop-gradient operator and ϵ' marks the new noise target. While MG eliminates sampling-time overhead of test-time guidance, it inherits CFG’s limitations in transfer learning and lacks a clear mechanism for allowing diversity-fidelity control at test time—a crucial principle in diffusion guidance.

Domain Guided Fine-Tuning

We propose DogFit, a training-time guidance mechanism for diffusion transfer learning that integrates a domain-aware guidance direction directly into the loss during fine-tuning. The marginal estimate of DogFit is derived from the unconditional source model (see Figure 3 (a-b)). DogFit modifies the training loss as:

$$\begin{aligned} \mathcal{L}_{\text{DogFit}} &= \mathbb{E}_{t, (x_0, c), \epsilon} \|\epsilon_{\theta}(x_t | c, \mathcal{D}^{\mathcal{T}}) - \epsilon'\|^2, \\ \epsilon' &= \epsilon + (w - 1) \cdot \text{sg}(\epsilon_{\theta}(x_t | c, \mathcal{D}^{\mathcal{T}}) - \epsilon_{\theta_0}(x_t)). \end{aligned} \quad (5)$$

The training architecture is illustrated in Figure 3(c). The training algorithm is shown in Appendix 4. The rest of this subsection provides theoretical insights motivating the design of DogFit (full statements and proofs are presented in Appendix 4).

Proposition 1. *Suppose a model is trained using the DogFit objective with controllable guidance strength w (Equation 6), and the following assumptions hold: (i) the model approximately recovers the true noise when no guidance is applied, and (ii) its predictions vary linearly with w . Then, for any value of w , the model replicates the effect of applying DoG at sampling time.*

Proposition 2. *DogFit is equivalent to implicitly applying a domain alignment component to MG’s training loss, benefiting from the class-conditional guidance of MG while reducing the risk of out-of-distribution generation.*

This means that ϵ_{θ_0} provides a strong and stable marginal noise estimate not only as an inference-time signal, but also during fine-tuning. Further, the domain alignment term, independent of class conditioning, pulls samples toward the core of the target data manifold, rendering DogFit effective even in the unconditional setting. In summary, DogFit, at its core, combines the strengths of previous guidance mechanisms in transfer learning into a single framework: it inherits the fast, single-pass sampling of MG and the robust marginal noise estimator of DoG.

Incorporating Controllability

A crucial feature of guidance is its controllability. To enable efficient fidelity–diversity trade-offs at test time, we introduce a lightweight conditioning mechanism to the model and treat w as an additional input condition during fine-tuning. The training objective with added control is:

$$\begin{aligned} \mathcal{L}_{\text{DogFit}} &= \mathbb{E}_{t, (x_0, c, w), \epsilon} \|\epsilon_{\theta}(x_t | c, w, \mathcal{D}^{\mathcal{T}}) - \epsilon'\|^2, \\ \epsilon' &= \epsilon + (w - 1) \cdot \text{sg}(\epsilon_{\theta}(x_t | c, 1, \mathcal{D}^{\mathcal{T}}) - \epsilon_{\theta_0}(x_t)), \end{aligned} \quad (6)$$

where $\epsilon_{\theta}(x_t | c, 1, \mathcal{D}^{\mathcal{T}})$ is the unguided class-conditional prediction. During training, the model must learn to operate across a range of guidance strengths to support controllable fidelity–diversity trade-offs at inference, while still preserving stable behavior in the unguided setting. Our initial experiments revealed that a simple uniform sampling of w during training can reduce diversity and destabilize generation, even at lower guidance levels due to excessive exposure to high w . Therefore, we sample w from a shifted exponential decaying distribution (see distribution CDF in Appendix 4):

$$w = 1 + z, \quad z \sim \mathcal{P}(z), \quad (7)$$

$$\mathcal{P}(z) = \lambda e^{-\lambda z}, \quad z \geq 0, \quad (8)$$

where λ controls the decay rate. This distribution favors smaller guidance strengths while occasionally introducing larger values, enabling guidance robustness without destabilizing training. As a result, the model generalizes well across the guidance spectrum and supports dynamic controllability

Table 1: FID and FD_{DINOv2} performance of DogFit against SOTA methods using DiT/XL-2 and SiT/XL-2 backbones. Their sampling costs are also shown in terms of forward passes and TFLOPs.

	Metric	Method	Unlabeled	Labeled						Sampling Cost	
			FFHQ	ArtBench	Caltech	CUB-Birds	Food	Stanford-Cars	Avg.	Passes	TFLOPs
DiT/XL-2	FID ↓	Fine-tuning	15.94	23.36	30.02	9.35	16.75	16.24	19.14	x1	366.14
		+ CFG (Ho and Salimans 2022)	-	20.83	24.07	5.03	11.77	10.60	14.46	x2	732.28
		+ DoG (Zhong et al. 2025)	13.87	17.30	23.76	3.65	10.97	<u>9.77</u>	13.09	x2	732.28
		MG (Tang et al. 2025)	-	19.91	23.71	4.85	11.13	11.03	14.13	x1	366.14
		DogFit	10.48	16.32	21.68	<u>3.69</u>	<u>10.64</u>	9.35	12.34	x1	366.14
		DogFit + Control	<u>13.03</u>	<u>16.98</u>	<u>21.98</u>	<u>3.69</u>	10.44	10.05	<u>12.63</u>	x1	366.14
	FD_{DINOv2} ↓	Fine-tuning	461.45	360.77	529.85	428.21	610.31	378.11	461.45	x1	366.14
		+ CFG (Ho and Salimans 2022)	-	314.32	401.96	200.92	410.48	227.46	311.03	x2	732.28
		+ DoG (Zhong et al. 2025)	273.93	<u>266.25</u>	<u>377.49</u>	135.74	314.16	132.91	245.31	x2	732.28
		MG (Tang et al. 2025)	-	299.06	409.20	220.40	379.39	255.88	312.78	x1	366.14
		DogFit	282.32	269.06	377.15	<u>143.42</u>	293.24	147.20	252.07	x1	366.14
		DogFit + Control	<u>274.67</u>	261.72	378.86	144.39	<u>314.12</u>	<u>141.08</u>	<u>248.03</u>	x1	366.14
SiT/XL-2	FID ↓	Fine-tuning	7.63	9.66	26.10	4.92	<u>7.76</u>	10.53	11.09	x1	454.01
		+ CFG (Ho and Salimans 2022)	-	<u>9.28</u>	<u>23.21</u>	<u>3.49</u>	7.95	<u>9.71</u>	<u>10.23</u>	x2	1083.77
		+ DoG (Zhong et al. 2025)	7.63	11.22	23.53	3.39	7.95	<u>9.71</u>	11.16	x2	1083.77
		MG (Tang et al. 2025)	-	9.64	23.10	3.60	<u>6.84</u>	8.62	9.94	x1	454.01
		DogFit	12.44	9.62	23.45	3.52	7.85	10.05	10.91	x1	454.01
		DogFit + Control	<u>10.8</u>	9.03	23.15	3.59	6.52	10.10	10.48	x1	454.01
	FD_{DINOv2} ↓	Fine-tuning	335.15	271.92	519.54	405.07	522.47	283.29	389.57	x1	454.01
		+ CFG (Ho and Salimans 2022)	-	236.13	406.63	203.47	368.26	190.24	280.94	x2	1083.77
		+ DoG (Zhong et al. 2025)	335.15	215.12	387.89	<u>160.85</u>	<u>298.65</u>	139.09	<u>240.32</u>	x2	1083.77
		MG (Tang et al. 2025)	-	232.17	418.86	229.32	359.90	203.23	297.16	x1	454.01
		DogFit	278.10	<u>222.20</u>	403.44	181.48	<u>296.49</u>	<u>159.83</u>	252.29	x1	454.01
		DogFit + Control	<u>319.16</u>	230.23	<u>399.20</u>	152.50	234.98	183.41	240.06	x1	454.01



Figure 4: Qualitative comparison of guidance mechanisms on DiT-XL/2 (guidance scale 1.5). \times : not applicable.

at inference (see Figure 5). The next key question is how to actually incorporate w into the model? In conditional diffusion models, the final condition embedding is typically formed by summing the label c and time-step t embeddings. Therefore, a natural approach to add w is to embed it and sum it with the other existing embeddings. However, we saw

that since the condition embedding propagates throughout the network and all layers are learnable, even slight distributional shifts and directional changes can destabilize training and disrupt the pretrained features. To avoid this, we use w as a label modulator: we embed it as a scalar, multiply it with the frozen label c embedding, and add the resulting modulation vector to the condition embedding. This design allows w to control the influence of the label without altering its semantic direction. This preserves the integrity of the pretrained embedding space and ensures stable guidance conditioning.

Guidance Scheduling Mechanisms

Inspired by recent advances in test-time guidance scheduling for improved generation quality (Sadat et al. 2023; Kynkäänniemi et al. 2024), we investigate the optimal timing and placement of training-time guidance using two simple yet effective strategies. First, we introduce a *late-start* mechanism that delays the injection of guidance until iteration $s > \tau_s$, thereby avoiding noisy updates and unstable gradients in the early phases of training. This is particularly beneficial in conditional settings where class embeddings are reinitialized to accommodate mismatched source and target label spaces. By deferring guidance, the model benefits from more stable target representations and condition embeddings, resulting in higher-fidelity updates. Second, we introduce a *cut-off* strategy that disables guidance at higher noise levels ($t > \tau_c$), concentrating domain su-

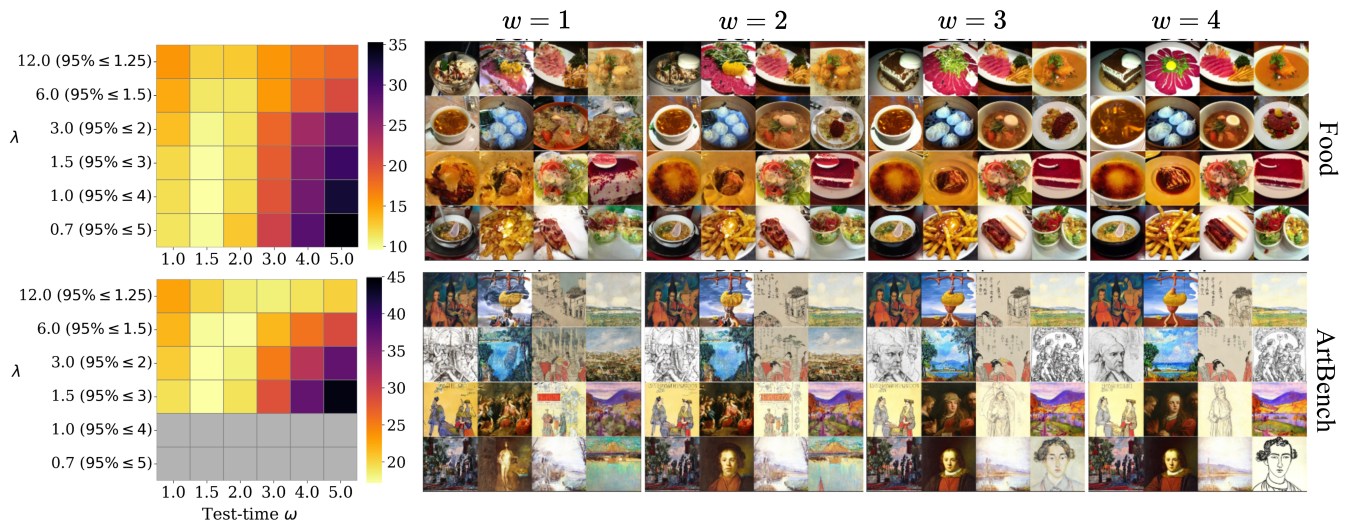


Figure 5: Effect of controllable guidance at test time for the Food and ArtBench domains. (Left) FID behavior across test-time w s with different training-time λ s. (Right) Corresponding generated samples for fixed $\lambda = 3$ (95% of sampled w values in $[1, 2]$), across varying test-time w . Gray cells indicate extreme FID values (≈ 350) resulting from collapsed generations.

pervision on the later denoising stages where adaptation to target-specific details is most effective (Choi et al. 2022). This design preserves source-driven diversity in the early denoising steps and prevents the model from over-relying on the target domain to shape the global structure of the image. This becomes crucial consideration when source and target domains share similar structural priors.

Results and Discussion

Setup. DogFit was validated on six challenging datasets with diverse domain characteristics and label availability for a comprehensive assessment: Food101 (Bossard, Guillaumin, and Van Gool 2014), Caltech101 (Griffin et al. 2007), CUB-200-201 (Wah et al. 2011), ArtBench10 (Liao et al. 2022), Stanford-Cars (Krause et al. 2013), and FFHQ256 (Karras, Laine, and Aila 2019). These datasets range from fine-grained species (Wah et al. 2011) to abstract art-styles (Liao et al. 2022) and face generation (Karras, Laine, and Aila 2019), covering a variety of distribution shifts in appearance, texture, and structure. We compare DogFit to standard fine-tuning, CFG, DoG, and MG. All methods are applied on DiT-XL/2 (Peebles and Xie 2023) and SiT-XL/2 (Ma et al. 2024) backbones pre-trained on ImageNet at 256×256 resolution for 7M steps with Fréchet Inception Distance (FID) (Heusel et al. 2017) scores of 2.27 (DiT) and 2.06 (SiT). We generate 10,000 images using 50 sampling steps (Peebles and Xie 2023; Xie et al. 2023), fixing the guidance strength to 1.5 for fair comparison, and fine-tune for 24,000 training steps (Zhong et al. 2025) with batch size of 32 on 2 A100 GPUs (40GB) for 5 hours. We calculate both FID (Heusel et al. 2017) and FD_{DINOv2} (Stein et al. 2023) between the generated images and the full datasets to evaluate the overall generation quality. Additionally, we compute Precision and Recall (Kynkäänniemi et al. 2019) for analyzing fidelity and diversity.

Comparison with State-of-the-art Methods

Table 1 summarizes our main quantitative findings. DogFit consistently performs comparatively or superior to prior methods in both FID and FD_{DINOv2} , while maintaining the efficiency of one-pass sampling. Unlike CFG and MG, DogFit remains effective in unconditional settings like FFHQ due to its class-agnostic domain-alignment direction. On SiT, CFG and MG slightly outperform DogFit in FID, but DogFit outperforms both CFG and MG on FD_{DINOv2} , underscoring the value of utilizing diverse metrics for comprehensive evaluation. Importantly, equipping DogFit with controllable guidance introduces no performance degradation while increasing the parameter count by only 1.33 million parameters (less than 2% of the initial network parameters), leaving no notable impact on sampling TFLOPS. Additional results on Precision and Recall are provided in Appendix 4. Figure 4 presents a visual comparison of generated samples across target domains on DiT. Guidance-based methods consistently outperform naïve fine-tuning by producing more realistic and coherent images. DogFit generates sharp, domain-relevant details on par with or better looking than DoG, while avoiding off-distribution artifacts occasionally seen with CFG and MG (e.g., distorted faces or tires). SiT qualitative results are provided in Appendix 4.

Ablation Studies

Controllable Guidance We study the effect of the decay rate hyperparameter λ used to sample the guidance scalar w during training (Equation 8). As shown in Figure 5 (left), sparse exposure to higher guidance is sufficient for generalization and achieving a diversity-fidelity tradeoff. In contrast, excessive exposure to large guidance can harm the model’s ability to retain pretrained features, leading to instability and collapsed generations. Based on these findings, we adopt $\lambda = 3$ (95% of sampled w s in $[1, 2]$) for all ex-

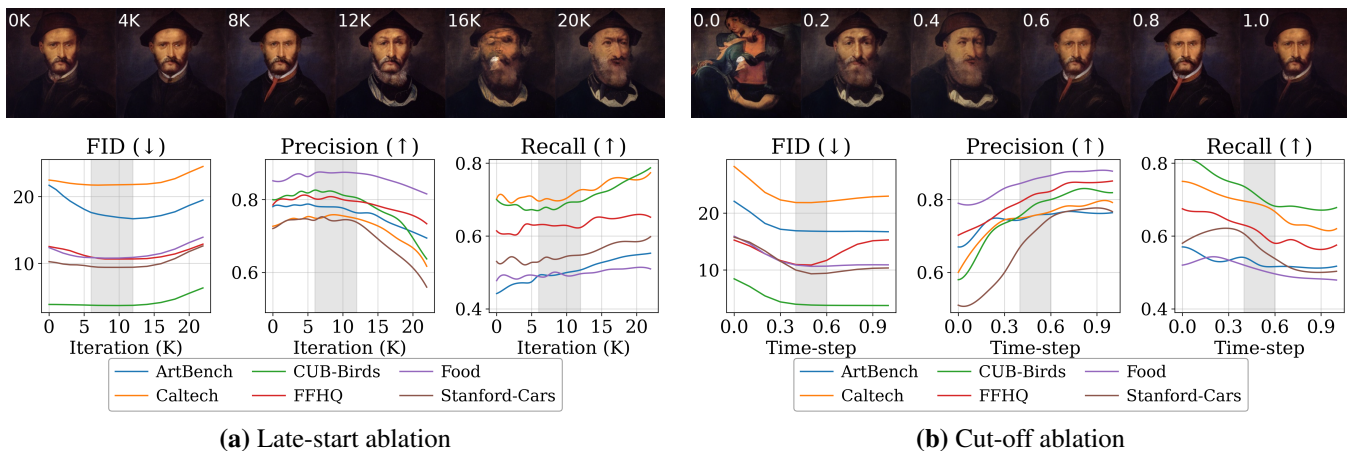


Figure 6: Ablation study on guidance schedules in DogFit. (a) Varying the late-start threshold τ_s to control when guidance begins. (b) Varying the cut-off threshold τ_c to restrict guidance to later denoising steps. Evaluation performed using FID.

Steps	Food		Art	
	MG	DogFit	MG	DogFit
10	60.60	57.91	108.26	88.84
25	21.13	18.97	39.80	29.11
50	11.13	10.64	19.91	16.32
100	7.60	8.09	13.38	12.70

Table 2: Sampling steps for MG and DogFit methods.

periments. Figure 5 (right) illustrates how varying guidance strength at test time effectively modulates the trade-off between fidelity and diversity, increasing sample quality while reducing variation with higher guidance values. For more analysis, see Appendix 4 and 4.

Guidance Scheduling. We analyze the impact of late-start and cut-off thresholds on generation quality and diversity. Figure 6(a) shows how varying the late-start threshold τ_s impacts FID, Precision, and Recall. Delaying guidance improves FID and especially Precision at first, as early stabilization allows formation of more accurate directional cues. However, setting τ_s too high leaves insufficient time for the model to internalize guidance, reducing it to naïve fine-tuning and lowering precision. We set $\tau_s = 12k$ for FID and $\tau_s = 6k$ for FD_{DINOv2} in all experiments. Figure 6(b) shows the effect of cut-off threshold τ_c on FID, Precision, and Recall. Delaying guidance to later denoising steps enhances diversity, particularly for target datasets with strong global structural similarity to the source domain, such as FFHQ, Cars, and Caltech. However, setting τ_c too low limits exposure to guidance, again reducing the model to naïve fine-tuning. While the optimal τ_c may depend on the source–target similarity, we use $\tau_c = 0.5$ for FID and $\tau_c = 1$ for FD_{DINOv2} in our experiments. See analysis on FD_{DINOv2} in Appendix 4.

Domain-guided Parameter-efficient Fine-tuning. We demonstrate that DogFit is fully compatible with DiffFit, a leading PEFT method for DiT models (Xie et al. 2023).

DiT-XL/2 Variant	FID↓		Train
	Food	Art	Params (M)
DogFit	10.64	16.32	675.42 (100%)
+ DiffFit	11.86	15.80	0.75 (0.11%)

Table 3: Combining DogFit with DiffFit.

As shown in Table 3, combining the two yields high-quality generations with lower cost in both training and test-time. This highlights DogFit’s practicality as a simple drop-in enhancement for efficient fine-tuning mechanisms.

Sampling Steps. Table 2 reports the effect of varying the number of sampling steps during generation. DogFit outperforms MG in nearly all settings, with especially notable gains at lower step counts. This underscores the effectiveness of DogFit’s target alignment in low-resource scenarios where fast sampling is critical.

Conclusion

In this paper, we introduce DogFit, a training-time guidance strategy for diffusion model transfer learning. It eliminates the high sampling-time cost of test-time guidance while preserving strong generalization behavior and controllability. DogFit leverages the pre-trained source model to inject high quality, domain-aligned guidance signals directly into the fine-tuning loss, and relies on a lightweight conditioning mechanism for inference fidelity–diversity adjustments. Our training-time guidance scheduling strategies further enhance training stability and generation quality. Extensive experiments across diverse target datasets and backbones show that DogFit can surpass the performance and efficiency of SOTA guidance methods, establishing it as a practical solution for scalable diffusion model transfer.

Limitations and Future Work. While effective, the proposed guidance scheduling strategies rely on manually chosen, fixed thresholds. Future work could explore adaptive or

data-driven approaches that respond to training dynamics or domain-specific properties. Moreover, although DogFit performs well on class-conditioned image domains, extending it to broader settings, i.e., text-to-image models, video generation, and other modalities, remains an exciting direction.

References

- Bossard, L.; Guillaumin, M.; and Van Gool, L. 2014. Food-101—mining discriminative components with random forests. In *Computer vision—ECCV 2014: 13th European conference, zurich, Switzerland, September 6–12, 2014, proceedings, part VI 13*, 446–461. Springer.
- Cao, Y.; and Gong, S. 2024. Few-shot image generation by conditional relaxing diffusion inversion. In *European Conference on Computer Vision*, 20–37. Springer.
- Chen, H.; Jiang, K.; Zheng, K.; Chen, J.; Su, H.; and Zhu, J. 2025. Visual Generation Without Guidance. *arXiv preprint arXiv:2501.15420*.
- Chen, M.; Huang, K.; Zhao, T.; and Wang, M. 2023. Score approximation, estimation and distribution recovery of diffusion models on low-dimensional data. In *International Conference on Machine Learning*, 4672–4712. PMLR.
- Choi, J.; Lee, J.; Shin, C.; Kim, S.; Kim, H.; and Yoon, S. 2022. Perception prioritized training of diffusion models. In *Proceedings of the IEEE/CVF Conference on Computer Vision and Pattern Recognition*, 11472–11481.
- Deja, K.; Kuzina, A.; Trzcinski, T.; and Tomczak, J. 2022. On analyzing generative and denoising capabilities of diffusion-based deep generative models. *Advances in Neural Information Processing Systems*, 35: 26218–26229.
- Dhariwal, P.; and Nichol, A. 2021. Diffusion models beat gans on image synthesis. *Advances in neural information processing systems*, 34: 8780–8794.
- Griffin, G.; Holub, A.; Perona, P.; et al. 2007. Caltech-256 object category dataset. Technical report, Technical Report 7694, California Institute of Technology Pasadena.
- Guo, D.; Rush, A. M.; and Kim, Y. 2020. Parameter-efficient transfer learning with diff pruning. *arXiv preprint arXiv:2012.07463*.
- Gupta, A.; Yu, L.; Sohn, K.; Gu, X.; Hahn, M.; Li, F.-F.; Essa, I.; Jiang, L.; and Lezama, J. 2024. Photorealistic video generation with diffusion models. In *European Conference on Computer Vision*, 393–411. Springer.
- Heusel, M.; Ramsauer, H.; Unterthiner, T.; Nessler, B.; and Hochreiter, S. 2017. Gans trained by a two time-scale update rule converge to a local nash equilibrium. *Advances in neural information processing systems*, 30.
- Ho, J.; Jain, A.; and Abbeel, P. 2020. Denoising diffusion probabilistic models. *Advances in neural information processing systems*, 33: 6840–6851.
- Ho, J.; and Salimans, T. 2022. Classifier-free diffusion guidance. *arXiv preprint arXiv:2207.12598*.
- Ho, J.; Salimans, T.; Gritsenko, A.; Chan, W.; Norouzi, M.; and Fleet, D. J. 2022. Video diffusion models. *Advances in Neural Information Processing Systems*, 35: 8633–8646.
- Hsiao, Y.-T.; Khodadadeh, S.; Duarte, K.; Lin, W.-A.; Qu, H.; Kwon, M.; and Kalarot, R. 2024. Plug-and-play diffusion distillation. In *Proceedings of the IEEE/CVF Conference on Computer Vision and Pattern Recognition*, 13743–13752.
- Hur, J.; Choi, J.; Han, G.; Lee, D.-J.; and Kim, J. 2024. Expanding expressiveness of diffusion models with limited data via self-distillation based fine-tuning. In *Proceedings of the IEEE/CVF Winter Conference on Applications of Computer Vision*, 5028–5037.
- Jensen, C. P.; and Sadat, S. 2025. Efficient Distillation of Classifier-Free Guidance using Adapters. *arXiv preprint arXiv:2503.07274*.
- Karras, T.; Aittala, M.; Kynkäänniemi, T.; Lehtinen, J.; Aila, T.; and Laine, S. 2024. Guiding a diffusion model with a bad version of itself. *Advances in Neural Information Processing Systems*, 37: 52996–53021.
- Karras, T.; Laine, S.; and Aila, T. 2019. A style-based generator architecture for generative adversarial networks. In *Proceedings of the IEEE/CVF conference on computer vision and pattern recognition*, 4401–4410.
- Kawar, B.; Zada, S.; Lang, O.; Tov, O.; Chang, H.; Dekel, T.; Mosseri, I.; and Irani, M. 2023. Imagic: Text-based real image editing with diffusion models. In *Proceedings of the IEEE/CVF conference on computer vision and pattern recognition*, 6007–6017.
- Krause, J.; Stark, M.; Deng, J.; and Fei-Fei, L. 2013. 3d object representations for fine-grained categorization. In *Proceedings of the IEEE international conference on computer vision workshops*, 554–561.
- Kynkäänniemi, T.; Aittala, M.; Karras, T.; Laine, S.; Aila, T.; and Lehtinen, J. 2024. Applying guidance in a limited interval improves sample and distribution quality in diffusion models. *arXiv preprint arXiv:2404.07724*.
- Kynkäänniemi, T.; Karras, T.; Laine, S.; Lehtinen, J.; and Aila, T. 2019. Improved precision and recall metric for assessing generative models. *Advances in neural information processing systems*, 32.
- Liao, P.; Li, X.; Liu, X.; and Keutzer, K. 2022. The art-bench dataset: Benchmarking generative models with artworks. *arXiv preprint arXiv:2206.11404*.
- Lu, C.; Zhou, Y.; Bao, F.; Chen, J.; Li, C.; and Zhu, J. 2022. Dpm-solver: A fast ode solver for diffusion probabilistic model sampling in around 10 steps. *Advances in Neural Information Processing Systems*, 35: 5775–5787.
- Ma, N.; Goldstein, M.; Albergo, M. S.; Boffi, N. M.; Vanden-Eijnden, E.; and Xie, S. 2024. Sit: Exploring flow and diffusion-based generative models with scalable interpolant transformers. In *European Conference on Computer Vision*, 23–40. Springer.
- Meng, C.; He, Y.; Song, Y.; Song, J.; Wu, J.; Zhu, J.-Y.; and Ermon, S. 2021. Sedit: Guided image synthesis and editing with stochastic differential equations. *arXiv preprint arXiv:2108.01073*.
- Moon, T.; Choi, M.; Lee, G.; Ha, J.-W.; and Lee, J. 2022. Fine-tuning diffusion models with limited data. In *NeurIPS 2022 Workshop on Score-Based Methods*.

Nichol, A.; Dhariwal, P.; Ramesh, A.; Shyam, P.; Mishkin, P.; McGrew, B.; Sutskever, I.; and Chen, M. 2021. Glide: Towards photorealistic image generation and editing with text-guided diffusion models. *arXiv preprint arXiv:2112.10741*.

Ouyang, Y.; Xie, L.; Zha, H.; and Cheng, G. 2024. Transfer Learning for Diffusion Models. *arXiv preprint arXiv:2405.16876*.

Peebles, W.; and Xie, S. 2023. Scalable diffusion models with transformers. In *Proceedings of the IEEE/CVF international conference on computer vision*, 4195–4205.

Phunyaphibarn, P.; Lee, P. Y.; Kim, J.; and Sung, M. 2025. Unconditional Priors Matter! Improving Conditional Generation of Fine-Tuned Diffusion Models. *arXiv preprint arXiv:2503.20240*.

Rombach, R.; Blattmann, A.; Lorenz, D.; Esser, P.; and Ommer, B. 2022. High-resolution image synthesis with latent diffusion models. In *Proceedings of the IEEE/CVF conference on computer vision and pattern recognition*, 10684–10695.

Sadat, S.; Buhmann, J.; Bradley, D.; Hilliges, O.; and Weber, R. M. 2023. CADs: Unleashing the diversity of diffusion models through condition-annealed sampling. *arXiv preprint arXiv:2310.17347*.

Salimans, T.; and Ho, J. 2022. Progressive distillation for fast sampling of diffusion models. *arXiv preprint arXiv:2202.00512*.

Shen, H.; Zhang, J.; Xiong, B.; Hu, R.; Chen, S.; Wan, Z.; Wang, X.; Zhang, Y.; Gong, Z.; Bao, G.; et al. 2025. Efficient Diffusion Models: A Survey. *arXiv preprint arXiv:2502.06805*.

Sohl-Dickstein, J.; Weiss, E.; Maheswaranathan, N.; and Ganguli, S. 2015. Deep unsupervised learning using nonequilibrium thermodynamics. In *International conference on machine learning*, 2256–2265. pmlr.

Song, J.; Meng, C.; and Ermon, S. 2020. Denoising diffusion implicit models. *arXiv preprint arXiv:2010.02502*.

Stein, G.; Cresswell, J.; Hosseinzadeh, R.; Sui, Y.; Ross, B.; Vिलецрозе, V.; Liu, Z.; Caterini, A. L.; Taylor, E.; and Loaiza-Ganem, G. 2023. Exposing flaws of generative model evaluation metrics and their unfair treatment of diffusion models. *Advances in Neural Information Processing Systems*, 36: 3732–3784.

Tang, Z.; Bao, J.; Chen, D.; and Guo, B. 2025. Diffusion Models without Classifier-free Guidance. *arXiv preprint arXiv:2502.12154*.

Wah, C.; Branson, S.; Welinder, P.; Perona, P.; and Belongie, S. 2011. The Caltech-UCSD Birds-200-2011 Dataset. Technical Report CNS-TR-2011-001, California Institute of Technology, Pasadena, CA, USA.

Wang, X.; Lin, B.; Liu, D.; Chen, Y.-C.; and Xu, C. 2024. Bridging data gaps in diffusion models with adversarial noise-based transfer learning. In *Forty-first International Conference on Machine Learning*.

Weiss, K.; Khoshgoftaar, T. M.; and Wang, D. 2016. A survey of transfer learning. *Journal of Big data*, 3: 1–40.

Xie, E.; Yao, L.; Shi, H.; Liu, Z.; Zhou, D.; Liu, Z.; Li, J.; and Li, Z. 2023. DiffFit: Unlocking transferability of large diffusion models via simple parameter-efficient fine-tuning. In *Proceedings of the IEEE/CVF International Conference on Computer Vision*, 4230–4239.

Yin, T.; Gharbi, M.; Zhang, R.; Shechtman, E.; Durand, F.; Freeman, W. T.; and Park, T. 2024. One-step diffusion with distribution matching distillation. In *Proceedings of the IEEE/CVF conference on computer vision and pattern recognition*, 6613–6623.

Zheng, C.; and Lan, Y. 2023. Characteristic guidance: Non-linear correction for diffusion model at large guidance scale. *arXiv preprint arXiv:2312.07586*.

Zheng, K.; Lu, C.; Chen, J.; and Zhu, J. 2023. Improved techniques for maximum likelihood estimation for diffusion odes. In *International Conference on Machine Learning*, 42363–42389. PMLR.

Zhong, J.; Guo, X.; Dong, J.; and Long, M. 2024. Diffusion tuning: Transferring diffusion models via chain of forgetting. *arXiv preprint arXiv:2406.00773*.

Zhong, J.; Zhang, X.; Wang, J.; and Long, M. 2025. Domain guidance: A simple transfer approach for a pre-trained diffusion model. *arXiv preprint arXiv:2504.01521*.

Zhou, Z.; Chen, D.; Wang, C.; Chen, C.; and Lyu, S. 2025. DICE: Distilling Classifier-Free Guidance into Text Embeddings. *arXiv preprint arXiv:2502.03726*.

Zhu, J.; Ma, H.; Chen, J.; and Yuan, J. 2022. Few-shot image generation with diffusion models. *arXiv preprint arXiv:2211.03264*.

Reproducibility Checklist

Instructions for Authors:

This document outlines key aspects for assessing reproducibility. Please provide your input by editing this `.tex` file directly.

For each question (that applies), replace the “Type your response here” text with your answer.

Example: If a question appears as

```
\question{Proofs of all novel claims
are included} {(yes/partial/no)}
Type your response here
```

you would change it to:

```
\question{Proofs of all novel claims
are included} {(yes/partial/no)}
yes
```

Please make sure to:

- Replace **ONLY** the “Type your response here” text and nothing else.
- Use one of the options listed for that question (e.g., **yes**, **no**, **partial**, or **NA**).

- **Not** modify any other part of the `\question` command or any other lines in this document.

You can `\input` this `.tex` file right before `\end{document}` of your main file or compile it as a stand-alone document. Check the instructions on your conference's website to see if you will be asked to provide this checklist with your paper or separately.

1. General Paper Structure

- 1.1. Includes a conceptual outline and/or pseudocode description of AI methods introduced (yes/partial/no/NA) **yes**
- 1.2. Clearly delineates statements that are opinions, hypothesis, and speculation from objective facts and results (yes/no) **yes**
- 1.3. Provides well-marked pedagogical references for less-familiar readers to gain background necessary to replicate the paper (yes/no) **yes**

2. Theoretical Contributions

- 2.1. Does this paper make theoretical contributions? (yes/no) **yes**

If yes, please address the following points:

- 2.2. All assumptions and restrictions are stated clearly and formally (yes/partial/no) **yes**
- 2.3. All novel claims are stated formally (e.g., in theorem statements) (yes/partial/no) **yes**
- 2.4. Proofs of all novel claims are included (yes/partial/no) **yes**
- 2.5. Proof sketches or intuitions are given for complex and/or novel results (yes/partial/no) **yes**
- 2.6. Appropriate citations to theoretical tools used are given (yes/partial/no) **yes**
- 2.7. All theoretical claims are demonstrated empirically to hold (yes/partial/no/NA) **yes**
- 2.8. All experimental code used to eliminate or disprove claims is included (yes/no/NA) **yes**

3. Dataset Usage

- 3.1. Does this paper rely on one or more datasets? (yes/no) **yes**

If yes, please address the following points:

- 3.2. A motivation is given for why the experiments are conducted on the selected datasets (yes/partial/no/NA) **yes**

- 3.3. All novel datasets introduced in this paper are included in a data appendix (yes/partial/no/NA) **NA**
- 3.4. All novel datasets introduced in this paper will be made publicly available upon publication of the paper with a license that allows free usage for research purposes (yes/partial/no/NA) **NA**
- 3.5. All datasets drawn from the existing literature (potentially including authors' own previously published work) are accompanied by appropriate citations (yes/no/NA) **yes**
- 3.6. All datasets drawn from the existing literature (potentially including authors' own previously published work) are publicly available (yes/partial/no/NA) **yes**
- 3.7. All datasets that are not publicly available are described in detail, with explanation why publicly available alternatives are not scientifically satisfying (yes/partial/no/NA) **NA**

4. Computational Experiments

- 4.1. Does this paper include computational experiments? (yes/no) **yes**

If yes, please address the following points:

- 4.2. This paper states the number and range of values tried per (hyper-) parameter during development of the paper, along with the criterion used for selecting the final parameter setting (yes/partial/no/NA) **no**
- 4.3. Any code required for pre-processing data is included in the appendix (yes/partial/no) **yes**
- 4.4. All source code required for conducting and analyzing the experiments is included in a code appendix (yes/partial/no) **yes**
- 4.5. All source code required for conducting and analyzing the experiments will be made publicly available upon publication of the paper with a license that allows free usage for research purposes (yes/partial/no) **yes**
- 4.6. All source code implementing new methods have comments detailing the implementation, with references to the paper where each step comes from (yes/partial/no) **yes**
- 4.7. If an algorithm depends on randomness, then the method used for setting seeds is described in a way sufficient to allow replication of results (yes/partial/no/NA) **yes**
- 4.8. This paper specifies the computing infrastructure used for running experiments (hardware and software), including GPU/CPU models; amount of memory; operating system; names and versions of

relevant software libraries and frameworks (yes/partial/no) **yes**

- 4.9. This paper formally describes evaluation metrics used and explains the motivation for choosing these metrics (yes/partial/no) **yes**
- 4.10. This paper states the number of algorithm runs used to compute each reported result (yes/no) **no**
- 4.11. Analysis of experiments goes beyond single-dimensional summaries of performance (e.g., average; median) to include measures of variation, confidence, or other distributional information (yes/no) **no**
- 4.12. The significance of any improvement or decrease in performance is judged using appropriate statistical tests (e.g., Wilcoxon signed-rank) (yes/partial/no) **no**
- 4.13. This paper lists all final (hyper-)parameters used for each model/algorithm in the paper's experiments (yes/partial/no/NA) **yes**

Appendix

Additional Methodology Explanations

DogFit Algorithm

Algorithm 1 summarizes the training loop of DogFit with controllability through guidance conditioning and the scheduling strategies.

Algorithm 1: DogFit training with Controllable Guidance and Scheduling

Require: Target dataset $\{\mathcal{D}^T\}$, noise schedule $\bar{\alpha}$, fixed source model ϵ_{θ_0} , training model ϵ_{θ} initialized by ϵ_{θ_0} , guidance cut-off τ_c , late-start step τ_s .

- 1: **for** training step $s = 1$ to S **do**
- 2: Sample target data $(x_0, c) \sim \{\mathcal{D}^T\}$
- 3: Sample noise $\epsilon \sim \mathcal{N}(0, 1)$ and time-step $t \sim \mathcal{U}(0, 1)$
- 4: Sample guidance strength $w = 1 + z$, $z \sim \mathcal{P}(z)$
- 5: Add noise: $x_t = \sqrt{\bar{\alpha}_t}x_0 + \sqrt{1 - \bar{\alpha}_t} \cdot \epsilon$
- 6: **if** $s > \tau_s$ **and** $t < \tau_c$ **then**
- 7: Compute guided target:
 $\epsilon' = \epsilon + (w - 1) \cdot \text{sg}(\epsilon_{\theta}(x_t | c, \mathbf{1}, \mathcal{D}^T) - \epsilon_{\theta_0}(x_t))$
- 8: **else**
- 9: $\epsilon' = \epsilon$
- 10: **end if**
- 11: Compute loss: $\mathcal{L}_{\text{DogFit}} = \|\epsilon_{\theta}(x_t | c, w, \mathcal{D}^T) - \epsilon'\|^2$
- 12: Backpropagate and update: $\theta = \theta - \eta \nabla_{\theta} \mathcal{L}_{\text{DogFit}}$
- 13: **end for**

CDF of Sampled Guidance Strengths

Figure 7 visualizes the Cumulative Distribution Function (CDF) of w s sampled during training from the exponentially decaying distribution in Equation 8. Larger values of λ concentrate the sampling mass closer to $w = 1$, limiting exposure to higher guidance values during training. This design ensures that the model primarily learns under weak to moderate guidance, while still sparsely encountering stronger guidance values.

Theoretical Insights into DogFit

In this section, we motivate the shift from using the marginal target noise estimate to the marginal source estimate in transfer learning. We discuss the benefits of this shift, and justify our method of applying it in the fine-tuning process. Then we show that under mild assumptions, DogFit learns to internalize DoG’s behaviour. Further, we conjecture that DogFit is an extension of MG, with an added domain alignment term.

General Assumptions. We assume that both the pretrained source model ϵ_{θ_0} and the fine-tuned model ϵ_{θ} share the same architecture and noise schedule (α_t), and are trained to approximate the same family of score functions under a common sampling procedure.

Guidance via Unconditional Source Prior The guidance signal in CFG is originally created via with the target domain conditional posterior $p_{\theta}(c | x_t, \mathcal{D}^T)$ to encourage sample

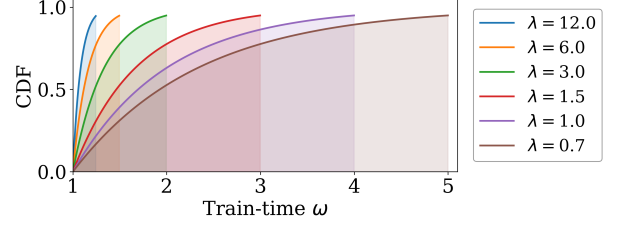


Figure 7: The CDF of sampled guidance strengths w during training for various λ values. The shaded region covers 95% of the samples.

fidelity and strong class-conditional alignment in the target domain. By Bayes’ rule:

$$p_{\theta}(c | x_t, \mathcal{D}^T) = \frac{p_{\theta}(x_t | c, \mathcal{D}^T) \cdot p_{\theta}(c | \mathcal{D}^T)}{p_{\theta}(x_t | \mathcal{D}^T)}, \quad (9)$$

or equivalently, in the log form:

$$\begin{aligned} \log p_{\theta}(c | x_t, \mathcal{D}^T) &= & (10) \\ \log p_{\theta}(x_t | c, \mathcal{D}^T) - \log p_{\theta}(x_t | \mathcal{D}^T) + \log p_{\theta}(c | \mathcal{D}^T). \end{aligned}$$

We consider the score functions (gradients of log-densities):

$$\begin{aligned} \nabla_{x_t} \log p_{\theta}(c | x_t, \mathcal{D}^T) &= & (11) \\ -\frac{1}{\sigma_t} (\nabla_{x_t} \log p_{\theta}(x_t | c, \mathcal{D}^T) - \nabla_{x_t} \log p_{\theta}(x_t | \mathcal{D}^T)), \end{aligned}$$

which are approximated by diffusion models:

$$\nabla_{x_t} \log p_{\theta}(x_t | c, \mathcal{D}^T) \approx -\frac{1}{\sigma_t} \epsilon_{\theta}(x_t | c, \mathcal{D}^T), \quad (12)$$

$$\nabla_{x_t} \log p_{\theta}(x_t | \mathcal{D}^T) \approx -\frac{1}{\sigma_t} \epsilon_{\theta_0}(x_t | \mathcal{D}^T). \quad (13)$$

Traditionally, CFG estimates both the class-conditional (Equation 12) and the marginal (Equation 13) noises with the same diffusion model. With enough data in the target domain, the class-conditional noise can be well estimated during fine-tuning via $\epsilon_{\theta}(x_t | c, \mathcal{D}^T)$. However, learning the target noise estimator $\epsilon_{\theta}(x_t | \mathcal{D}^T)$ faces the risk of undertraining due to only being trained on a small portion of the small target dataset. Since the source model is usually trained on large, diverse datasets, it likely captures a good approximation of the general image manifold. Furthermore, it has been shown that diffusion models have generalizability on other data distributions (Deja et al. 2022) and can denoise noisy images from domains other than those they have been trained on (Meng et al. 2021). Therefore, we can assume that the pre-trained source model captures a general enough prior, giving us the ability to approximate the unconditional score using the pre-trained source model, leading to the formulation of DoG:

$$\nabla_{x_t} \log p_{\theta}(x_t | \mathcal{D}^T) \approx -\frac{1}{\sigma_t} \epsilon_{\theta_0}(x_t). \quad (14)$$

Thus, the posterior score can be approximated as:

$$\nabla_{x_t} \log p_\theta(c | x_t, \mathcal{D}^\mathcal{T}) \propto -\frac{1}{\sigma_t} (\epsilon_\theta(x_t | c, \mathcal{D}^\mathcal{T}) - \epsilon_{\theta_0}(x_t)), \quad (15)$$

which exactly matches the offset used in DoG sampling (Zhong et al. 2025). Our method takes a step further from this and applies the same guidance offset online. We train a diffusion model to directly predict this guided score instead of separately learning Equations 12 and 13 in the form of DoG.

Proposition 1. Let $\epsilon_\theta(x_t | c, w)$ be the DogFit model with controllable guidance trained with the objective:

$$\mathcal{L}_{\text{DogFit}} = \|\epsilon_\theta(x_t | c, w, \mathcal{D}^\mathcal{T}) - (\epsilon + (w - 1) \cdot \Delta(x_t, c, \mathcal{D}^\mathcal{T}))\|^2, \quad (16)$$

where $\Delta(x_t, c, \mathcal{D}^\mathcal{T}) = \epsilon_\theta(x_t | c, w = 1, \mathcal{D}^\mathcal{T}) - \epsilon_{\theta_0}(x_t)$ and assume the following conditions hold after convergence:

- (i) When no guidance is applied, the model approximately recovers the true noise ϵ used in training.
- (ii) The model’s prediction varies linearly with the guidance strength w .

Then for any w , the DogFit model matches the DoG-guided score used at sampling time:

$$\begin{aligned} \epsilon_\theta(x_t | c, w, \mathcal{D}^\mathcal{T}) &= \\ \epsilon_\theta(x_t | c, \mathcal{D}^\mathcal{T}) + (w - 1) \cdot (\epsilon_\theta(x_t | c, \mathcal{D}^\mathcal{T}) - \epsilon_{\theta_0}(x_t)). \end{aligned} \quad (17)$$

Note on the assumptions: Prior work on CFG has shown that the linearity assumption holds in practice for low to moderate w values (Zheng and Lan 2023). Furthermore, our use of an exponentially decaying distribution to sample w during training (see Section) helps maintain accurate estimation of ϵ in the unconditional setting. Based on this, we conjecture that both assumptions can approximately hold in practice.

Proof sketch. At convergence, the DogFit objective minimizes the expected loss:

$$\mathbb{E}_{x_0, t, \epsilon, w} \left[\|\epsilon_\theta(x_t | c, w, \mathcal{D}^\mathcal{T}) - (\epsilon + (w - 1) \cdot \Delta(x_t, c, \mathcal{D}^\mathcal{T}))\|^2 \right]. \quad (18)$$

Assuming that $\epsilon_\theta(x_t | c, w)$ is linear in w , we can write the model as:

$$\epsilon_\theta(x_t | c, w, \mathcal{D}^\mathcal{T}) = A + B \cdot (w - 1). \quad (19)$$

Since the training loss is a squared error between two linear functions of w , minimizing this loss for all values of w is equivalent to matching the corresponding coefficients of both functions. That is, to minimize the loss over the full support of w , the model must satisfy:

$$A = \epsilon, \quad B = \Delta(x_t, c, \mathcal{D}^\mathcal{T}). \quad (20)$$

Since $\epsilon_\theta(x_t | c, \mathcal{D}^\mathcal{T}) \approx \epsilon_\theta(x_t | c, w = 1, \mathcal{D}^\mathcal{T}) \approx \epsilon$, this gives the optimal solution:

$$\epsilon_\theta(x_t | c, w, \mathcal{D}^\mathcal{T}) = \epsilon + (w - 1) \cdot (\epsilon_\theta(x_t | c, \mathcal{D}^\mathcal{T}) - \epsilon_{\theta_0}(x_t)), \quad (21)$$

which is exactly the DoG-guided prediction used at test time. Therefore, DogFit learns to internalize the DoG guidance signal during training, removing the need for external guidance at sampling. ■

Proposition 2. DogFit implicitly augments MG’s training process with a classifier-based domain alignment term:

$$\epsilon'_{\text{DogFit}} = \epsilon'_{\text{MG}} - \sigma(w - 1) \cdot \nabla_{x_t} \log p_\theta(\mathcal{D}^\mathcal{T} | x_t). \quad (22)$$

This enables DogFit to retain MG’s class-conditional guidance while avoiding out-of-distribution generation by pulling samples toward the core of the target domain manifold.

Proof sketch. The target noise in MG, when applied in the task of fine-tuning, can be rewritten as:

$$\epsilon'_{\text{MG}} = \epsilon + (w - 1) \cdot \text{sg}(\epsilon_\theta(x_t | c, \mathcal{D}^\mathcal{T}) - \epsilon_\theta(x_t | \mathcal{D}^\mathcal{T})). \quad (23)$$

Then, by subtracting the target noise values of MG and DogFit, we have:

$$\epsilon'_{\text{DogFit}} - \epsilon'_{\text{MG}} = (w - 1) \cdot \text{sg}(\epsilon_\theta(x_t | \mathcal{D}^\mathcal{T}) - \epsilon_{\theta_0}(x_t)). \quad (24)$$

According to Equations 12 and 13, Equation 24 can be rewritten as:

$$= -\sigma(w - 1) \cdot \text{sg}(\nabla_{x_t} \log p_\theta(x_t | \mathcal{D}^\mathcal{T}) - \nabla_{x_t} \log p_\theta(x_t)) \quad (25)$$

By Bayes’ rule, we have:

$$\frac{p(x_t | \mathcal{D}^\mathcal{T})}{p(x_t)} \propto p(\mathcal{D}^\mathcal{T} | x_t), \quad (26)$$

which is equivalent to:

$$\nabla_{x_t} \log p(\mathcal{D}^\mathcal{T} | x_t) = \nabla_{x_t} \log p_t(x_t | \mathcal{D}^\mathcal{T}) - \nabla_{x_t} \log p_t(x_t). \quad (27)$$

Thus, given that MG uses $\epsilon_\theta(x_t | \mathcal{D}^\mathcal{T})$ as an approximation to $-\sigma_t \nabla_{x_t} \log p(x_t | \mathcal{D}^\mathcal{T})$, we can express DogFit as applying MG, but with a correction term that pushes towards a target domain classifier’s gradient direction. ■

Additional Experiments

FID sensitivity to w without Controllability

We further examine the sensitivity of our method to w in the absence of controllability. We train a specific model for each w and compare the FID trends of DogFit and DoG across varying values (Figure 10). While both methods achieve optimal FID in a similar range, DogFit exhibits a sharper degradation for larger w , suggesting higher sensitivity to strong guidance values. We hypothesize that this is due to training-time overexposure to extreme guidance, which can lead the model to learn from unnatural signals that do not follow the real target distribution, thereby reducing generation quality. This motivates our design choice in Section to sample w from an exponentially decaying distribution, ensuring the model is only sparsely exposed to high guidance values during training.

Controllable Guidance Analysis on Cars

Figure 8 provides an extended version of the controllable guidance analysis for the Stanford-Cars dataset. This complements the main findings and illustrates the same trends on a new domain.

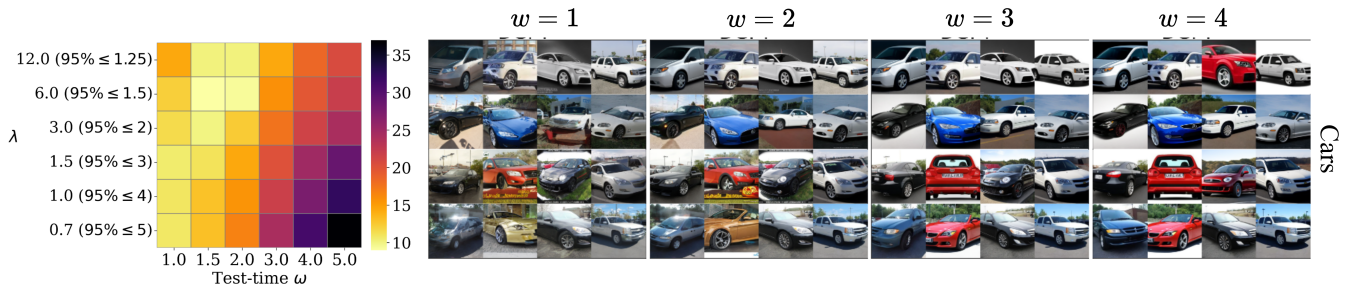


Figure 8: Effect of controllable guidance at test time for the Stanford-Cars domain. (Left) FID heatmaps showing the behaviour of FID given different test-time w s with different training-time λ s. (Right) Corresponding generated samples for fixed $\lambda = 3$ (i.e., 95% of sampled w values lie between 1 and 2), across varying test-time w .

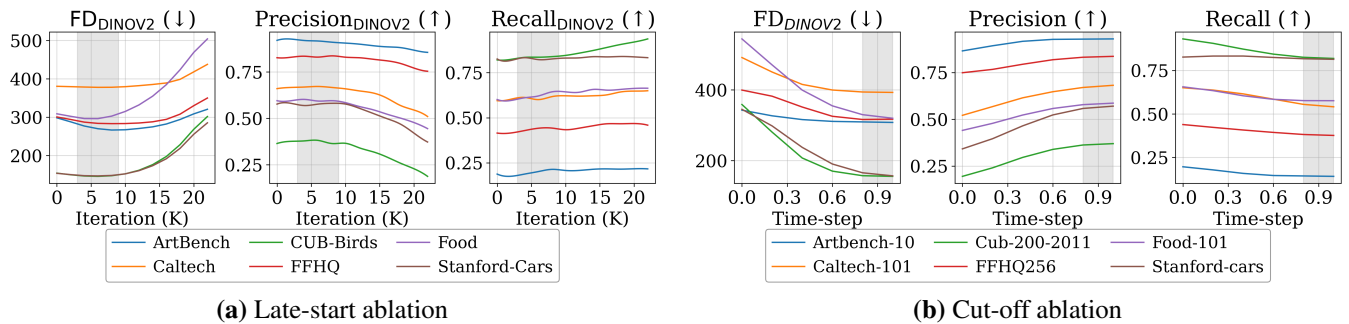


Figure 9: Ablation study on guidance schedules in DogFit. (a) Varying the late-start threshold τ_s to control when guidance begins. (b) Varying the cut-off threshold τ_c to restrict guidance to later denoising steps. Evaluation performed using FD_{DINOv2} .

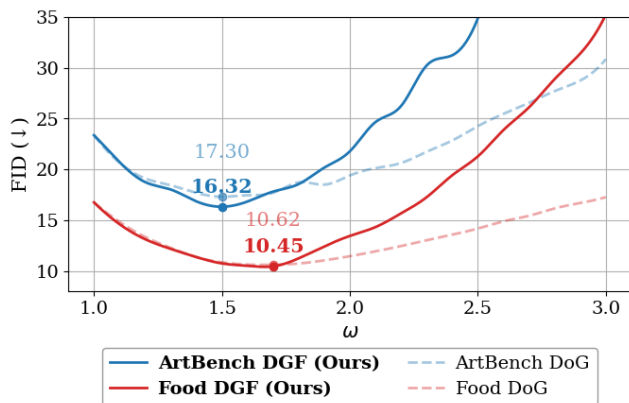


Figure 10: Comparing DogFit (without guidance control) and DoG in sensitivity of FID to w .

Guidance Scheduling on FD_{DINOv2}

We observe that delaying guidance using the late-start strategy improves both FD_{DINOv2} and precision, consistent with our FID-based findings. This supports the idea that postponing guidance allows for stronger and more accurate directional signals once the model has sufficiently stabilized (Figure 9a). However, unlike FID, applying the cut-off strategy—where guidance is limited to later denoising steps—shows little to no improvement in FD_{DINOv2}

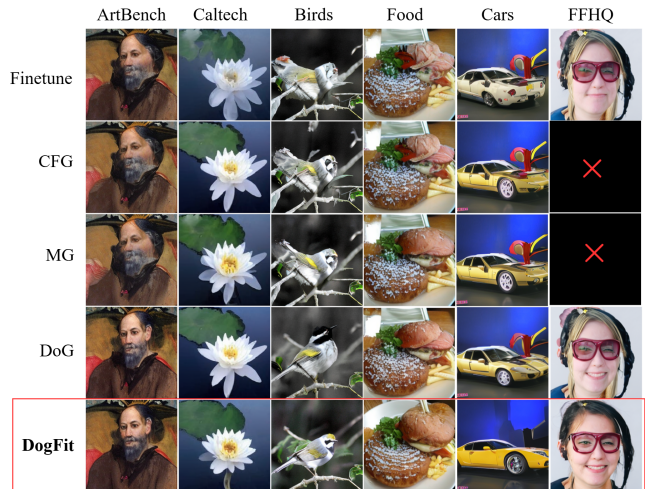


Figure 11: Qualitative comparison of guidance mechanisms on SiT-XL/2 (guidance scale 1.5). \times : not applicable.

across most domains (Figure 9 (b)). We believe this is due to a fundamental difference in what the two metrics capture: FID benefits from preserving the global structure inherited from the source model, which is often formed early in the denoising process. In contrast, FD_{DINOv2} focuses more on semantic alignment with the target domain, which may re-

quire guidance to be present throughout the generation, not just in the later steps. This distinction further highlights the importance of using multiple metrics when evaluating generative models.

Qualitative Comparison on SiT-XL/2

Figure 11 provides a qualitative comparison on the SiT-XL/2 backbone. DogFit generates sharp, domain-relevant details on par with DoG, while avoiding out-of-distribution behavior occasionally seen with CFG and MG (e.g., distorted faces and birds).

Precision and Recall Analysis

Table 4 presents a comparison of Precision and Recall (Kynkäänniemi et al. 2019) between DogFit and the baselines on the DiT-XL/2 backbone. Precision reflects the fidelity or quality of generated samples, while Recall measures sample diversity. As expected, all guidance methods consistently improve Precision compared to finetuning while reducing Recall, aligning with the general behavior of guided diffusion models. This effect arises because guidance steers sampling toward high-likelihood regions of the conditional distribution, which inherently narrows the output distribution and suppresses diversity. Our method, both with and without guidance control, matches the performance of DoG in terms of both Precision and Recall in most settings. Notably, DogFit achieves the highest or second-highest Precision in both Inception and DINOv2 metrics across all datasets). In terms of Recall, DogFit and DoG slightly underperform CFG and MG, which we believe is due to the additional domain alignment term further reducing the diversity to prevent out-of-domain target generations (Equation 22). While recent works explore diversity-preserving techniques and scheduling mechanisms for guidance during sampling (Kynkäänniemi et al. 2024; Sadat et al. 2023), analogous techniques for training-time guidance have yet to be developed. We leave the exploration of such methods for training-guided models like DogFit as an exciting direction for future work.

Table 4: Precision and Recall results on DiT/XL-2 backbone using Inception and DINOv2 metrics.

Metric	Method	Unlabelled	Labelled					
		FFHQ	ArtBench	Caltech	CUB-Birds	Food	Stanford-Cars	Avg.
Precision (Inception)	Fine-tuning	0.70	0.67	0.60	0.58	0.79	0.51	0.63
	+ CFG (Ho and Salimans 2022)	-	0.68	0.76	0.72	0.82	0.63	0.72
	+ DoG (Zhong et al. 2025)	0.83	0.77	0.81	<u>0.82</u>	0.88	<u>0.77</u>	0.81
	MG (Tang et al. 2025)	-	0.68	0.76	0.71	0.81	0.62	0.72
	DogFit	<u>0.81</u>	<u>0.76</u>	0.75	<u>0.82</u>	<u>0.87</u>	0.74	<u>0.79</u>
	DogFit + Control	0.83	<u>0.76</u>	<u>0.78</u>	0.83	<u>0.87</u>	0.80	0.81
Precision (DINOv2)	Fine-tuning	0.74	0.84	0.48	0.16	0.41	0.30	0.44
	+ CFG (Ho and Salimans 2022)	-	0.83	<u>0.67</u>	0.30	0.48	0.47	0.52
	+ DoG (Zhong et al. 2025)	0.82	<u>0.91</u>	0.73	0.39	0.59	0.61	0.65
	MG (Tang et al. 2025)	-	0.84	0.63	0.28	0.51	0.44	0.54
	DogFit	<u>0.83</u>	0.92	<u>0.67</u>	<u>0.38</u>	<u>0.58</u>	0.58	<u>0.62</u>
	DogFit + Control	0.86	0.90	<u>0.67</u>	<u>0.38</u>	<u>0.58</u>	<u>0.59</u>	<u>0.62</u>
Recall (Inception)	Fine-tuning	0.67	0.57	0.75	0.81	0.52	<u>0.58</u>	0.65
	+ CFG (Ho and Salimans 2022)	-	<u>0.56</u>	0.66	<u>0.76</u>	<u>0.53</u>	0.59	0.62
	+ DoG (Zhong et al. 2025)	0.61	0.50	0.65	0.68	0.48	0.52	0.57
	MG (Tang et al. 2025)	-	<u>0.56</u>	0.67	0.75	0.55	0.59	<u>0.624</u>
	DogFit	<u>0.63</u>	0.51	<u>0.70</u>	0.68	0.50	0.55	0.59
	DogFit + Control	0.57	0.51	0.68	0.67	0.50	0.48	0.57
Recall (DINOv2)	Fine-tuning	0.46	0.21	0.66	0.95	0.67	0.82	0.66
	+ CFG (Ho and Salimans 2022)	-	0.22	0.59	0.87	0.61	0.84	<u>0.63</u>
	+ DoG (Zhong et al. 2025)	<u>0.44</u>	0.21	0.57	0.83	<u>0.64</u>	0.83	0.62
	MG (Tang et al. 2025)	-	0.22	0.60	0.89	0.60	0.84	<u>0.63</u>
	DogFit	0.43	0.21	0.60	0.83	<u>0.64</u>	0.83	0.62
	DogFit + Control	0.43	0.21	<u>0.61</u>	0.85	<u>0.64</u>	0.83	<u>0.63</u>